

Effect of the Heating Rate and Processing Time on Grain Growth of Hematite Nanopowders in Conventional and Microwave-Assisted Sintering

Marina Magro Togashi^{a*} , Claudia Patricia Fernandez Perdomo^a , Ruth H.G.A. Kiminami^a 

^aUniversidade Federal de São Carlos, Programa de Pós-Graduação em Ciência e Engenharia de Materiais, Rodovia Washington Luiz, km 235 SP-310, 13565-905, São Carlos, SP, Brasil.

Received: January 15, 2023; Revised: April 12, 2023; Accepted: July 19, 2023

Microwave-assisted sintering of ceramic materials has proven to be a very favorable processing technique that can promote lower grain growth and densification with shorter dwell times. Hematite is considered a good microwave absorber due to its high loss tangent value, calculated in the range of 0.001 to 0.2 between room temperature and 750 °C for 2.45 GHz¹, thus showing good interaction with this electromagnetic radiation. However, there are few studies on grain growth kinetics of hematite during microwave sintering, as well as the relationship with grain growth parameters. Therefore, the aim of this work was to evaluate the effect of the heating rate and dwell time on grain growth kinetics, during microwave-assisted sintering (2.45 GHz) of hematite nanopowders. In an initial characterization, dilatometry tests were performed by conventional heating and microwave-assisted heating using the same heating rate (20 °C/min). From these results, the temperature ranges of the initial and intermediate stages of sintering and the onset of linear shrinkage were determined. Considering these results, the samples were sintered in a conventional oven from 750 °C to 1200 °C with increments of 50 °C, varying the dwell time in 6, 12 and 36 minutes. Thus, the diffusional mechanism (N) could be calculated, a value used for the approximate calculation of microwave sintering kinetics. Additionally, sintering was performed in a microwave oven using three heating rates (20, 30 and 50 °C/min) to evaluate the effect of the heating rate on grain growth. The estimated activation energies for the grain growth process during microwave sintering were approximately 237.5 to 272.3 kJ/mol, which were higher compared to conventional sintering, in the range of 206.0 to 242.0 kJ/mol. It was found that with increasing microwave heating rate, the activation energy for grain growth tends to be higher.

Keywords: *Microwave sintering kinetics, Hematite nanopowders, Grain growth kinetics.*

1. Introduction

Hematite (α -Fe₂O₃) is the most stable phase of iron oxide, the crystalline structure of the material belongs to the rhombohedral system^{1,2,3}. Hematite has excellent properties at room temperature, providing the material with good chemical stability, good catalytic activity, excellent gas sensitivity properties and superparamagnetism⁴. Thus, hematite has applications in many fields such as pigments, cosmetics², application in medical area⁴, gas and humidity sensors³, electrochemical and photocatalyst sensors^{5,6}.

The particle size and its morphology are determinant in properties and applications of the material. Nanotechnology has been widely studied in recent years due to the unique properties that can be achieved^{3,7}. The synthesis of iron oxide nanoparticles can be done for several routes, highlighting the chemical routes, which ensure lower average particle sizes, high purity and reproducibility. Many studies have been reported on the synthesis of nanohematite by routes such as sol-gel^{2,7,8}, Pechini⁶, gel combustion, melted salt method⁵, electrochemical deposition, solvothermal and hydrothermal³.

The great challenge found in this context is the nanometric scale retention after the ceramic powder

sintering step, even with nanometric starting powders. In this scenario, the microwave-assisted sintering is a great alternative to overcome this challenge, as it promotes volumetric heating and allows the use of ultrafast heating rates (100 - 150 °C/min), when compared to conventional sintering^{9,10}. Discovered during the second world war, microwave radiation was first used in the food sector. The processing of ceramic materials using microwave radiation started to be studied in the 1960s and 1970s as it offers many benefits. Among them, volumetric heating mentioned above stands out. Regardless of the sample complexity combined with the shorter processing time, the densification of most materials occurs at lower temperatures when compared to the conventional process, and lower global energy spent in the full heating cycle. However, some challenges still remain especially regarding the comprehension of the parameters and thermodynamic mechanisms during the heating and ultrafast microwave-assisted sintering⁸⁻¹¹.

The capacity for the material to be polarized, and thus heated, is dependent on dielectric properties, intrinsic to the material, according to Equation 1. The loss tangent is represented for $\tan \delta$, and the real and complex permittivity for ϵ' and ϵ'' , respectively¹¹.

*e-mail: mtogashi@ppgcecm.ufscar.br

$$\tan \delta = \frac{\epsilon''}{\epsilon'} \quad (1)$$

The complex permittivity is associated with the energy dissipation processes in the form of heat, therefore it is the parameter related to the material's capacity to be microwave heated, while the real permittivity is associated with the dielectric constant. Thus, a material with higher loss tangents has higher values of complex permittivity, which results in a better microwave absorber or is easily heated by microwaves^{11,12}. In the literature, the hematite is reported as a good absorber of microwave energy, presenting relatively high loss tangent values. The $\tan \delta$ values, calculated for hematite nanopowders (30 nm) in this work, are in the range of 0.001 to 0.2 between room temperature up to 750 °C for a frequency of 2.45 GHz¹². Consequently, the material shows high electromagnetic radiation absorption, especially in the electrical field^{11,13-15}.

In this context, the kinetic studies are necessary for a better understanding of the heating through electromagnetic radiation, calculating the thermodynamical parameter. Thus, it is also possible to carry out optimization in the processing. Considering isothermal conditions, the activation energy can be calculated for grain growth (Ea)¹⁶, according to Equation 2:

$$G^N - G_0^N = K_0 t e^{\left(-\frac{Ea}{RT}\right)} \quad (2)$$

Where G is the grain size, G_0 the initial particle size, K_0 a pre-exponential factor, N the diffusional coefficient, T the absolute temperature, t the sintering time and R the universal gas constant, which is 8.31 J/(mol*K). The value of N was calculated in this work for hematite nanopowders in the conventional sintering and it was used as the base value for the calculation of grain growth energy in microwave sintering.

Equation 2 can be reduced to Equation 3, assuming that the initial particle size is much smaller than the final grain size.

$$\log \frac{G^N}{t} = \log K_0 - \frac{0,434Ea}{RT} \quad (3)$$

The curve $\log (G^N/t)$ versus $1/T$ has an angular coefficient $(0.434 Ea)/R$. Thus, it is used in the activation energy calculation for the grain growth process during material sintering¹⁶.

Kinetics studies on microwave sintering, both for densification and grain growth, are recent and still scarce. They were reported in many conditions for ceramic materials such as: ZnO¹⁷, graphene, zirconia and alumina composites¹⁸ and iron and titanium oxides¹⁵, and these authors used isothermal methods, based on linear shrinkage data of the compounds, in the case of α -alumina¹⁹, NiCuZn ferrite²⁰ in which they used the non-isothermal method for densification kinetics. This method was also used for hematite nanopowders, according to our last publication for densification kinetics in 2.45 GHz²¹. The present study aims to evaluate the effect of the heating type, heating rate and processing time in the kinetic grain growth during sintered hematite nanopowders.

2. Experimental Procedure

The nanometric iron oxide in the hematite phase was obtained by modified sol-gel synthesis using polyacrylic acid as the chelating agent as reported in a previous study²¹. The initial particle size of the hematite starting powder was estimated at 30 nm. Figure 1 shows the TEM micrograph, X-ray diffraction pattern and the particle size distribution with Lognormal fit. The micrograph analysis showed spherical particles with high agglomeration, typical of nanopowders.

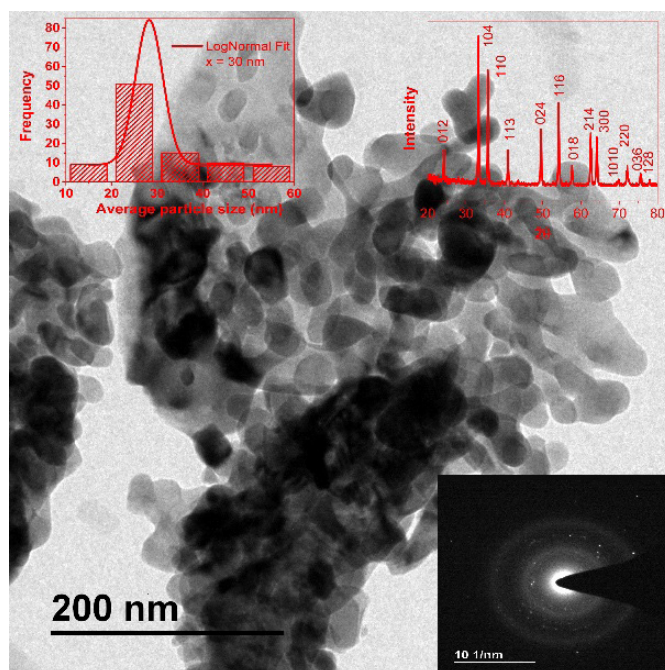


Figure 1. TEM micrograph of the starting powder of hematite (30 nm).

The X-ray pattern indicates the high crystallinity of the nanopowder. The particle size distribution indicates narrow particle size distribution. All of this was corroborated with the specific surface area estimated with the results of the BET technique. The area was estimated at 28.6 m²/g and the equivalent diameter was 40 nm, close to TEM estimation²¹.

Initially, the samples were conformed by cold uniaxial pressing in a hydraulic press with a 200 MPa load. The samples for dilatometry were conformed in a bar shape with a square transversal section, with approximate dimensions of 10x3x3 mm. The green densities were calculated using the geometric method, considering 5.24 g/cm³ as the theoretical density. The geometric method consists of measuring the length, width and thickness with a caliper rule. The multiplication of the data is the geometric volume. The geometric density is the mass of the sample divided by the geometric volume. In this way, the theoretical density is the maximum density achieved by hematite according to the literature, which would correspond to 100% of densification. The compacts were submitted to dilatometries in a conventional oven in a NETZSCH DIL 420C horizontal dilatometer, and in a microwave-assisted dilatometer, comprising a horizontal contact dilatometer Linseis platinum series L75HX1000/1600 coupled to a semi-industrial microwave oven with multimodal cavity Linn MKH4.8. The heating rate used was 20 °C/min aiming to observe the behavior of the linear shrinkage of hematite submitted to the conventional and microwave heating and the thermodynamical parameters as the onset of shrinkage and final stage of sintering.

Cylindric shape samples were also conformed separately by cold uniaxial pressing in a hydraulic press and load of 200 MPa with dimensions of 5.5 mm in diameter and 3 mm in length. The green densities were also calculated using the geometric method. Then, the compacts were sintered in a conventional oven and in a microwave oven. A Cober Electronics MS6K semi-industrial furnace was used, with an operating frequency of 2.45 GHz and a maximum power of 1.8 kW, with heating rates of 20, 30 and 50 °C/min and the dwell time of 5 minutes. For the sake of comparison, a Lindberg Blue M oven was used for conventional sintering. For both cases, the sintering temperature was used ranging from 850 °C to 1200 °C with increments of 50 °C. During the conventional heating cycle, a heating rate was used of 5 °C/min until 400 °C and then 20 °C/min up to the final temperature. The dwell times were 6, 12 and 36 minutes, aiming to calculate the diffusional mechanism (N) for conventional sintering. The same N value was used for microwave sintering. All the experiments were made in triplicate to guarantee the reproducibility of the experiment.

The apparent density was measured using the immersion method, following the Archimedes principle, according to the ABNT NBR 6620 standard, and microstructural characterizations were carried out, in which the fractured/polished surface was analyzed and thermally attacked at 50 °C below the temperature of sintering for 15 minutes to reveal the grains and grain boundaries in the samples. The average grain size was determined using the planimetric grain size method by calculating the number of grains per unit length using the Image J software. The kinetics study was carried out using isothermal models of grain growth, according to Equation 2 and Equation 3.

3. Results and Discussions

3.1. Dilatometry

Initially, the samples were conformed in a bar shape with a transversal square section, and they had the value of green density in approximately 42% of the theoretical density. The samples were submitted to the conventional oven and assisted microwave at 2.45 GHz oven dilatometries. The density increased as a function of the temperature and the shrinkage decreased, as expected for both types of heating. The dilatometric curves with a heating rate of 20 °C/min and final temperature of 1150 °C of the nanometric hematite are presented in Figure 2.

The final relative densities after the conventional and microwave dilatometries were approximately 86.1% and 86.0%, respectively. These values were calculated by the immersion method. Regarding the graph through the densification curve, the value reaches approximately 85.3% and 85.0%, respectively. These values were slightly different, as they are instantaneous densification values, calculated by Equation 4.

$$\rho = \frac{\rho_0}{\left(1 + \frac{\Delta l}{l_0}\right)^3} \quad (4)$$

In which ρ_0 is the initial density of the compact, ρ is the instantaneous density and $\Delta l/l_0$, the linear shrinkage.

By Equation 4, it is possible to perceive an inversely proportional variation between linear shrinkage and instantaneous density, thus, as there was greater densification with the use of microwave energy, it is possible to perceive greater linear shrinkage, when compared to conventional heating. It can be observed that the linear shrinkage is slightly higher in microwave-assisted sintering, when compared to conventional sintering at the same temperature as observed in Figure 2.

Moreover, a large difference can be observed between the linear shrinkage curves above 600 °C. Thus, differences in important processing temperatures can be inferred: onset temperatures of shrinkage, maximum linear shrinkage rate, initial and intermediate stage range of sintering. These differences are described in Table 1.

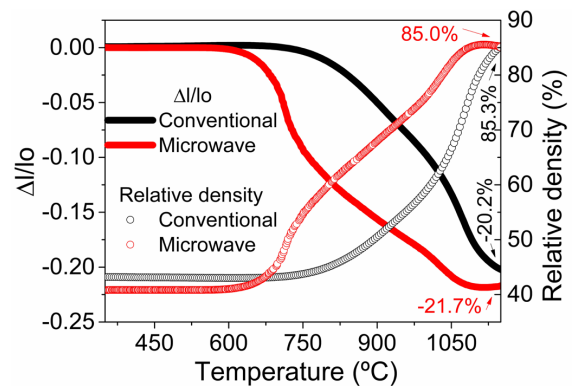


Figure 2. Curve of linear shrinkage and instantaneous relative density as a function of temperature for the nanometric hematite compacts submitted to conventional and microwave dilatometries with a heating rate of 20 °C/min.

A decrease of approximately 85 °C in the onset temperature of shrinkage can be observed, which indicates that the linear shrinkage begins before in the microwave-assisted sintering. Croquesel et al.²² verified the reduction of the onset temperature of shrinkage of alumina powder when sintered by microwave in a single mode cavity. The authors attributed this decrease of temperature to the ponderomotive forces. This force comes from the action of the electromagnetic field and is an additional driving force to the sintering process. Thus, the authors proposed that these forces are able to increase the surface and grain boundary diffusion, in the case of alumina, accelerating the mass transport processes.

The range of initial and intermediate stages of hematite also occurs in lower temperatures, indicating the acceleration of diffusional processes in the whole process of microwave sintering, especially at the beginning of the process.

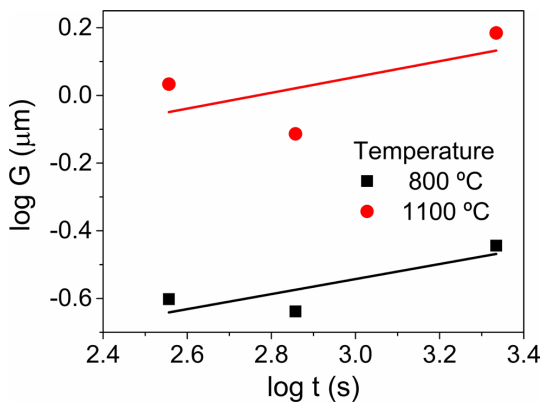


Figure 3. Graphic of the grain size vs dwell time of the hematite sintered conventionally at 20 °C/min.

This was reported by Rybakov et al.¹⁰ who demonstrated the higher acceleration of the initial stage kinetics for densification of ceramic materials.

3.2. Calculus of the diffusional mechanism during conventional sintering

The kinetics study for grain growth during conventional sintering of hematite nanopowders was performed aiming to estimate the diffusional mechanism (N) of the processing. The conformed nanopowders in cylindrical shape were submitted to conventional sintering at temperatures from 750 °C to 1200 °C, with increments of 50 °C. The heating rate was 20 °C/min and the dwell times were 6, 12 and 36 minutes for each isotherm. Considering the temperatures of 800 °C and 1100 °C, the diffusional mechanism (N) was calculated through the graphic in Figure 3 below.

The value of the diffusional mechanism corresponds to the slope of the curve in Figure 3 calculated for the temperature of 800 °C that was 3.2 and for the temperature of 1100 °C it was 1.6. Thus, for the calculus of activation energy, the intermediate value of 3.2 was used.

Figure 4 shows the correspondent micrographs of the dots in the graphic in Figure 3. Figure 5 illustrates the respective distribution histograms of the average grain size. An approach to a Lognormal curve was used.

In Figure 4, the increase in the value of the average grain size can be observed with the increase in the sintering temperature. Furthermore, at the same temperature, there is an increase in the average grain size, with an increase in the dwell time. This tendency was observed in Figure 3 and corroborated with Figure 4. By analyzing Figure 5, a tendency of a narrower distribution of average grain size for the temperature of 800 °C can be observed compared to 1100 °C. Furthermore, there is a tendency of a narrower distribution for the lower dwell times.

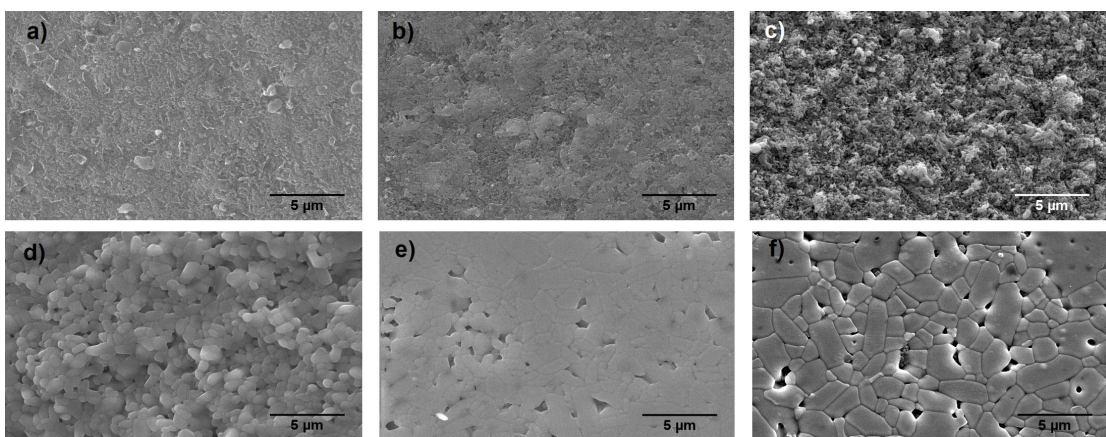


Figure 4. Micrographs of the conventionally sintered hematite with a heating rate of 20 °C/min up to 800 °C and dwell times of a) 6, b) 12 and c) 36 minutes. Up to 1100 °C and dwell times of d) 6, e) 12 and f) 36 minutes.

Table 1. Conventional and microwave dilatometry parameters with heating rate of 20 °C/min.

Type of heating	Onset temperature of shrinkage (°C)	Range of initial stage (°C)	Range of intermediate stage (°C)
Conventional	675	800-890	890-1180
Microwave	590	620-685	685-1115

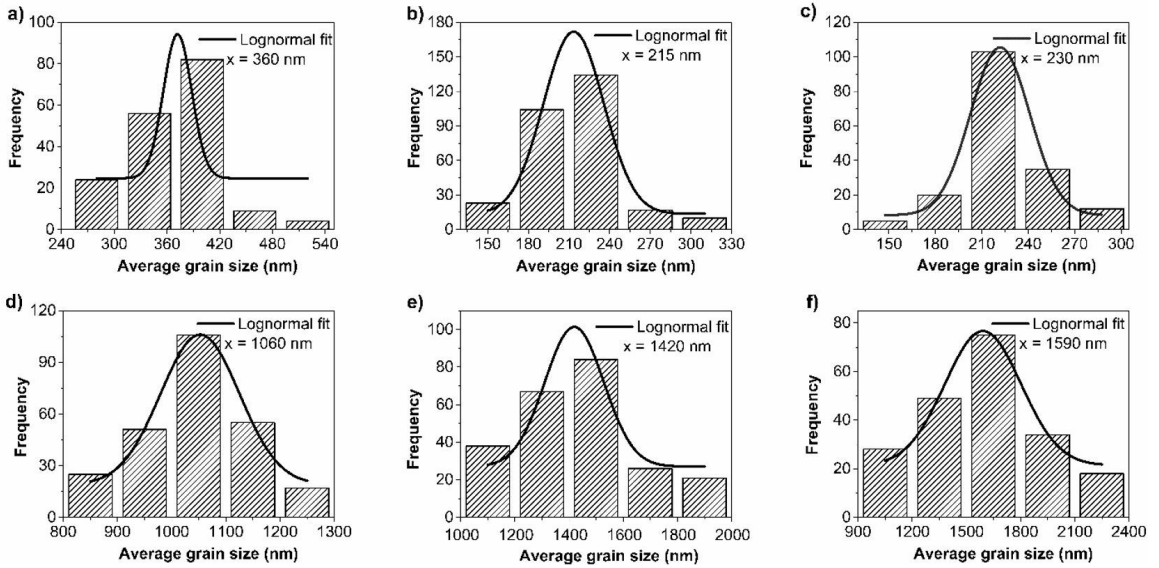


Figure 5. Distribution histograms of the average grain size of conventionally sintered hematite with a heating rate of 20 °C/min up to 800 °C with dwell times of a) 6, b) 12 and c) 36 minutes. Up to 1100 °C with dwell times of d) 6, e) 12 and f) 36 minutes.

Table 2 presents the activation energy values calculated for the conventional sintering of hematite as a function of the dwell times, as well as the value of the average grain size at 1200 °C, which was the highest temperature used in this case.

The values of activation energy for grain growth of the hematite during conventional sintering were calculated using Equation 2 and Equation 3, and they are in the range of 205 to 242 kJ/mol. The highest dwell time is related to the lower energy needed for grain growth, corroborated with the higher grain growth for the higher dwell times. This tendency was reported by Nuernberg and Morelli²³ for a BSCF ferrite with a perovskite structure, in which the authors observed that both the relative density and the grain size depend on the dwell time, in conventional and microwave sintering.

3.3. Kinetics study of the grain growth during microwave sintering

The grain growth study was performed during the microwave-assisted sintering of hematite at 2.45 GHz. The initial green density of the compacts was approximately 47%. The densification increased with the increase in temperature, as expected as it is a thermally activated process. Regarding the processing time, the heating cycle in the microwave sintering was faster than in the conventional sintering. Despite using the same final temperature, the heating rate in the microwave was 20 °C/min, while in the conventional, it was necessary to heat at 5 °C/min up to 400 °C, due to the thermal inertia of the oven and then it was heated at 20 °C/min. Thus, only in the heating cycle was there a two-fold reduction in the processing time. This reduction was even bigger during the cooling cycle. There was an acceleration in the cooling process by up to 10 times. This occurred since in microwave sintering only the sample was heated and not all the oven components, unlike what occurs in conventional sintering, in which the furnace components are heated to heat the sample.

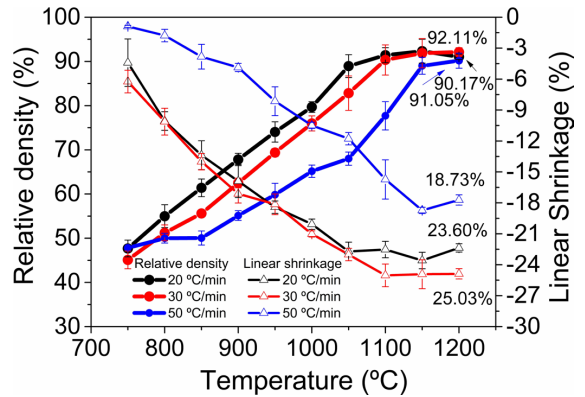


Figure 6. Relative density and linear shrinkage as a function of temperature in the microwave-assisted sintering of the hematite NPs with an initial particle size of 30 nm and with heating rates of 20 °C/min, 30 °C/min and 50 °C/min.

Table 2. Activation energies (E_a) calculated by the grain growth method during conventional sintering of hematite nanopowders with a heating rate of 20 °C/min and final average grain size at the end of the processing.

Dwell time	E_a (kJ/mol)	Average grain size (μm)
6 min	228.5	2.3
12 min	242.0	2.5
36 min	205.6	2.5

This results in an almost 80% decrease in the overall processing time. Figure 6 compares relative density and linear shrinkage as a function of temperature and heating rate. Rates of 20, 30 and 50 °C/min and a dwell time of 5 minutes were used.

In the curves in Figure 6, a significant increase in the densification rate from 750 °C can be observed reaching a stable value in 1150 °C in the heating rate of 50 °C/min and in 1100 °C, for the slower rates of 20 and 30 °C/min, with densifications of approximately 90% of relative density. Thus, this first difference with the higher heating rate can be observed, once its linear shrinkage values (18.7%) were lower, compared to the rates of 20 and 30 °C/min (23.6% and 25.0%, respectively). The densification and linear shrinkage values were analyzed and combined with the grain growth data to comprehend

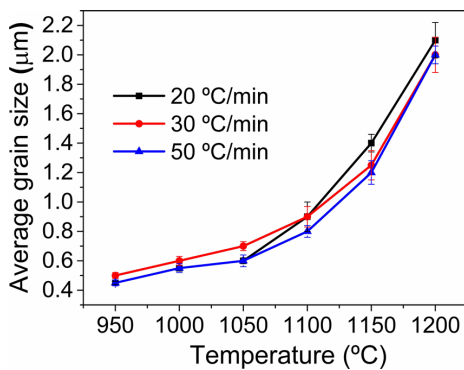


Figure 7. Graphic of the average grain size as a function of the temperature and heating rate during microwave-assisted sintering of the hematite.

the global phenomenon of the kinetic effect of microwave sintering of the nano-hematite. The error bars in Figure 6 were calculated by the deviation of the triplicate values. They show the deviation in the statics data obtained. The errors corroborate the reliability of the data.

Figure 7 presents the graphic with the evolution of the grain size as a function of the temperature and heating rate. The tendency of smaller grain sizes with the increase in temperature was confirmed. The microstructures will be presented next.

By analyzing the graphic, a slight tendency of lower values of average grain size can be observed with the increase in the heating rate. In this case, grain sizes were obtained of 2.0, 1.9 and 1.8 μm for the rates of 20, 30 and 50 °C/min, respectively, with a final temperature of 1200 °C. A tendency of lower grain sizes with the increase in the heating rate was observed for the zinc oxide by Gunnewiek and Kiminami¹⁷. The authors observed that the heating rate altered the grain growth of the zinc oxide during microwave sintering, when rates of 50, 75 and 100 °C/min were used. The authors obtained finer microstructures with higher heating rates. However, since the hematite is a good absorber of the microwave radiation, this strong tendency was not observed in this work.

The microstructural analysis is presented next. In the micrographs in Figure 8, the evolution of the grain size can be seen as a function of the temperature, for the heating rate of 20 °C/min, clearly observing the growth of the grains with the increase in temperature.

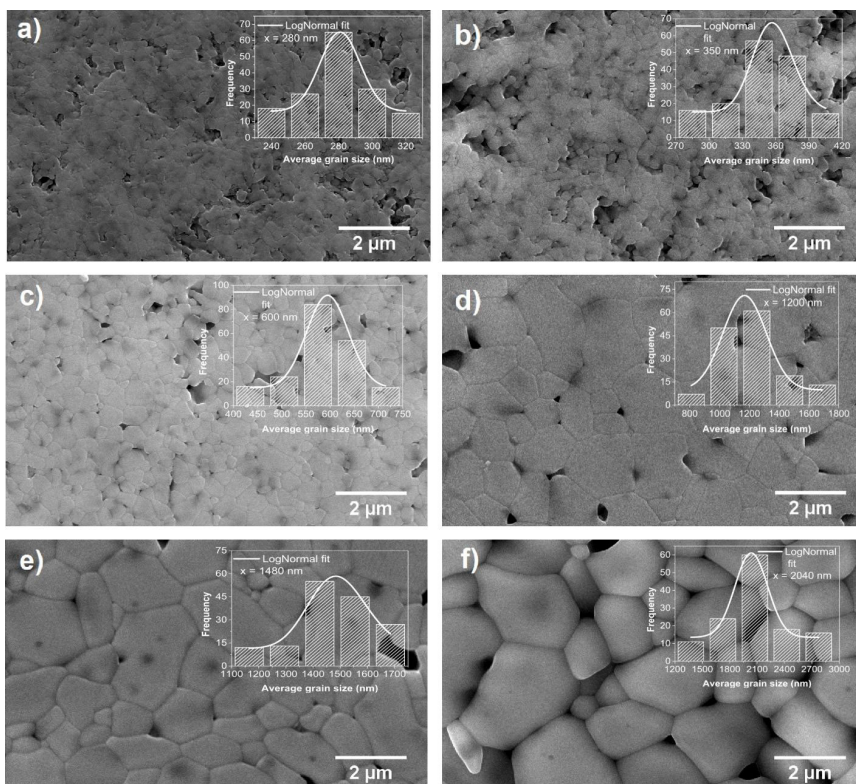


Figure 8. Micrographs of microwave sintered nano-hematite with heating rate 20 °C/min, and dwell time of 5 minutes at a) 950 °C, b) 1000 °C, c) 1050 °C, d) 1100 °C, e) 1150 °C and f) 1200 °C (Histograms inset).

It can be noted that at 950 °C, the neck formation is complete, indicating that this temperature corresponds to the intermediate stage of sintering. Thus, it can be inferred that there is an accelerated increase in the densification rate above 950 °C. These data are corroborated to that predicted in the microwave dilatometry characterization in 20 °C/min, in which the range of temperatures of the initial stage of sintering corresponds from 800 °C to 890 °C, and the intermediate stage, from 890 °C to 1180 °C, according to that presented in Table 1. A final average grain size of 2.0 μm, at 1200 °C was observed, indicating the favoring of the diffusional processes for grain growth, typical of the final stage of sintering and final density of 91% at this temperature.

A notable grain growth between 1100 °C and 1200 °C can be observed, which corresponds with that observed in Figure 6, with a lower densification rate from 1100 °C. This can indicate that the densification was already complete since then, and there was a predominance of grain growth mechanisms. It is known that during the sintering process there is a strong competition between densification and grain growth. As the driving force is the same for both processes, the diminution of the energy is associated with the surfaces²⁴.

In the micrographs of Figure 9, the microstructural evolution was observed in 30 °C/min. The final density values were 92% and the average grain size was 1.9 μm, both at 1200 °C. These values are very similar to those obtained in 20 °C/min.

It can be also noted that at 950 °C, the neck formation is complete, which is an indication that in this temperature, the material is already in the intermediate stage of sintering

at microwave. A notable grain growth can also be observed between 1100 °C and 1200 °C, which corresponds to the lower densification rate from 1100 °C, as discussed previously.

In the micrographs of Figure 10, the microstructural evolution in 50 °C/min can be observed. The values of the final density and average grain size in 1200 °C were 90% and 1.8 μm, respectively.

It can be also noted that at 950 °C and 1000 °C, the neck formation is complete, which is an indication that in this temperature, the material is already in the intermediate stage of sintering at microwave. A notable grain growth can also be observed between 1100 °C and 1150 °C, which corresponds to the lower densification rate from 1150 °C. This result indicates a displacement in the initial and intermediate stages for higher temperatures when the hematite is submitted to high rates in the microwave sintering. At 1200 °C, the final average grain size was 1.8 μm, similar to what was obtained in the same temperatures using averages rates of sintering (20 °C/min and 30 °C/min).

This accelerated growth may be linked to the fact that the material is already very dense, and the supply of more energy only causes grain growth and no longer densification. In addition, the grain growth in the case of nanostructured hematite when sintered by microwaves does not strongly depend on the sintering rate. The system can be submitted to fast and ultrafast sintering to obtain ceramic bodies with similar characteristics of densification and grain growth to the obtained using average rates of sintering, which is reflected in consequent energy saving.

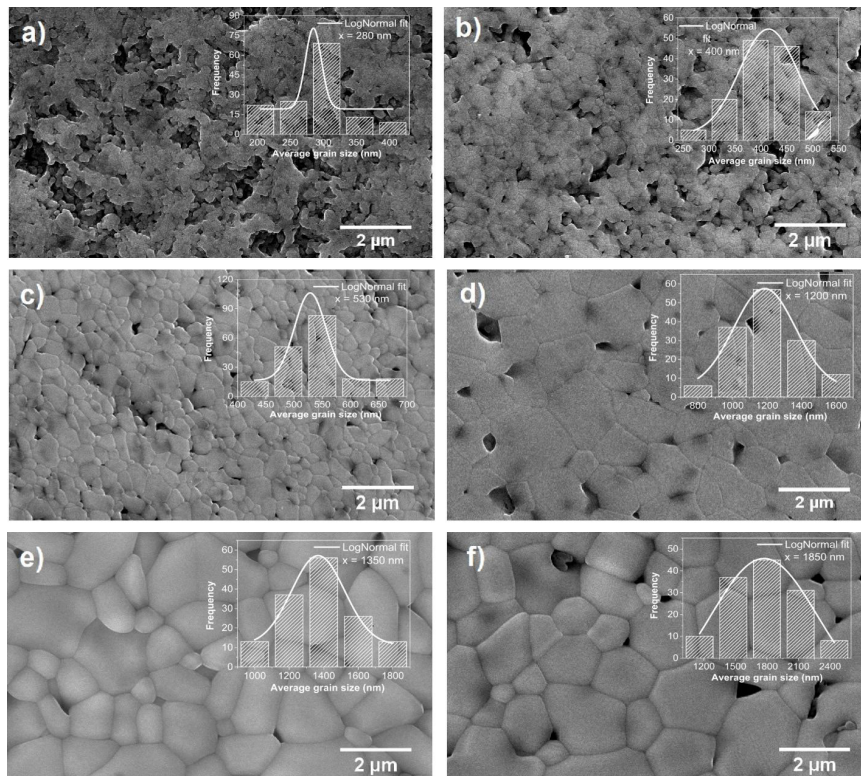


Figure 9. Micrographs of microwave sintered nano-hematite with a heating rate 30 °C/min, and dwell time of 5 minutes at a) 950 °C, b) 1000 °C, c) 1050 °C, d) 1100 °C, e) 1150 °C and f) 1200 °C (Histograms inset).

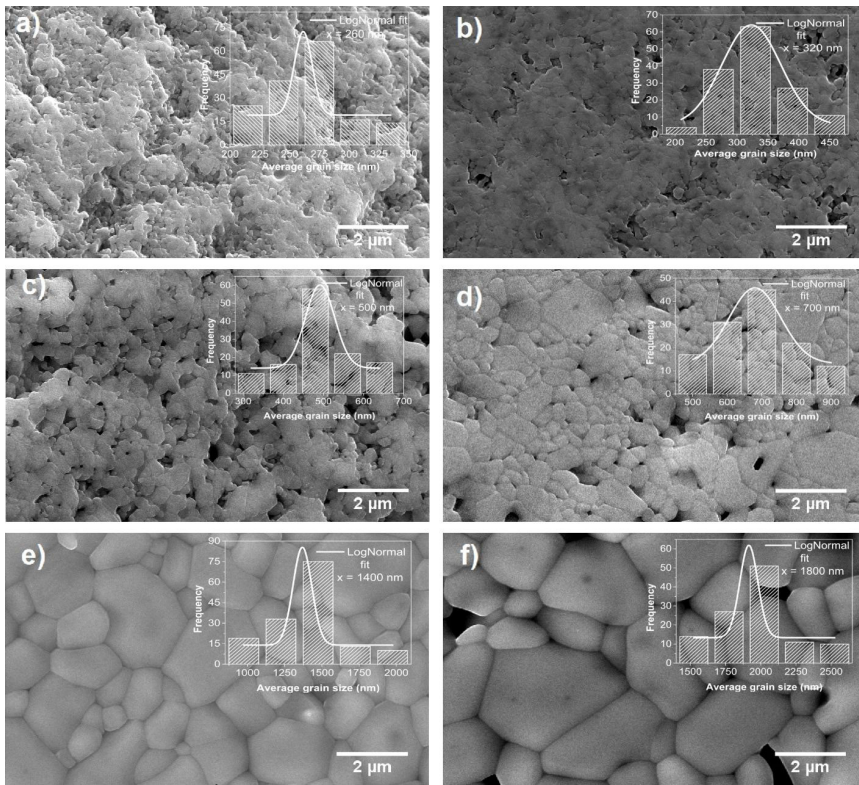


Figure 10. Micrographs of microwave sintered nano-hematite with a heating rate 50 °C/min, and dwell time of 5 minutes at a) 950 °C, b) 1000 °C, c) 1050 °C, d) 1100 °C, e) 1150 °C and f) 1200 °C (Histograms inset).

Since the hematite is a good absorber of the microwave energy, the studies related to hematite nanopowders focus on their use as dopants or additives. Some works with nanometric hematite focus more on the synthesis part using microwave radiation. There are some microwave processing studies for nanometer ferrites. Zhu et al.²⁰ studied NiCuZn ferrite, and the method used in that study was the use of a CCD camera to verify shrinkage. In this case, conventional and microwave heating were compared, and it was observed that, with microwave energy, the activation energy calculated by the sintering master curve was reduced by 100 - 150 kJ.

Next, in Figure 11, the Arrhenius graphs of $\log(G^N/t)$ versus $1/T$ and Table 3 with the calculated values of the activation energy of grain growth through isothermal methods of grain growth are presented, considering an intermediate diffusional mechanism of 3.2, as calculated for the conventional sintering of this powder, assuming that the diffusional mechanism is not altered with the application of microwave energy.

Table 3. Activation energy for grain growth calculated for the hematite as a function of the heating rate.

Heating rate	Ea (kJ/mol)	Grain size (μm)
20 °C/min	244.0	2.0
30 °C/min	237.5	1.9
50 °C/min	272.3	1.8

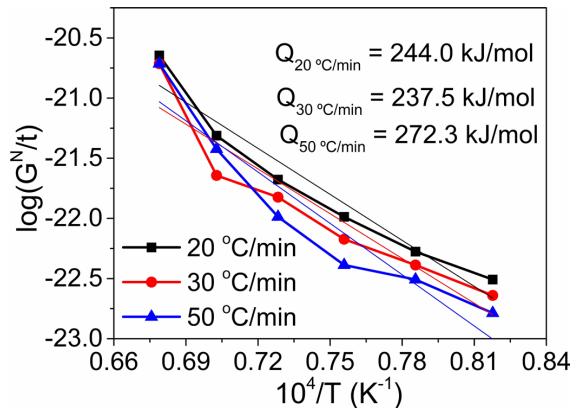


Figure 11. Arrhenius plot of $\log(G^N/t)$ versus $10^4/T$ for the sintered hematite with heating rates of 20, 30 and 50 °C/min.

Table 3 presents the values of activation energy for grain growth with the corresponding heating rate and final grain size obtained at 1200 °C, which was the highest temperature used in this work.

There is a tendency towards higher activation energy values for higher heating rates, which means that it is necessary to provide the system with greater thermal energy to favor the diffusion mechanisms for grain growth, which translates into a retention of grain growth when the heating rate is increased even though hematite is a highly

microwave absorbing material, which is corroborated by the lower grain growth, as previously discussed. At 1200 °C, the grains exceeded the nanometric scale, due to the excess energy used. As seen previously, at lower temperatures, the densification of the samples was sufficient for potential future applications, such as gas and humidity sensors, electrochemical and photocatalyst sensors. Compared with conventional sintering, activation energy values for grain growth are in the range of 206 – 242 kJ/mol (Table 2), and are lower than those obtained in microwave sintering, indicating that by conventional heating less thermal energy is required to initiate grain growth mechanisms.

There are no data in the literature about the activation energy for grain growth during microwave sintering of hematite. However, it is possible to find values for other ceramic materials. As reported by Gunnewiek and Kiminami¹⁷ for the zinc oxide. The authors calculated activation energy values for grain growth during microwave sintering in the range from 254 kJ/mol to 388 kJ/mol, with heating rates of 50, 75 and 100 °C/min. Du et al.²⁵ reported values for an alumina composite. The values were calculated in the range from 361.2 kJ/mol to 423.3 kJ/mol, depending on the niobium oxide amount added.

4. Conclusions

The effect of heating rate and processing time in grain growth sintering kinetics of nanohematite was evaluated for microwave and conventional sintering. Activation energy values for grain growth were calculated during microwave sintering of hematite, with the initial particle size of 30 nm, between 237.5 to 272.3 kJ/mol. For the calculus, a diffusional mechanism of 3.2 was used, calculated through the grain growth kinetics for the hematite in conventional sintering. Compared to conventional sintering, in which, the energy was calculated in the range of 206.0 to 242.0 kJ/mol, it can be inferred that higher energy is needed for the grain growth process during microwave sintering and consequently the grain growth is reduced. This was data corroborated by the smallest average grain size by processing with microwave energy. Therefore, this study showed unprecedented values for the grain growth kinetics of the hematite for microwave sintering.

5. Acknowledgments

The authors would like to thank FAPESP n. process 2017/13769-1, CNPq n. processes 305129/2018-0 and 165313/2017-0 and CAPES n. process 88882.332729/2019-01 for the financial support and scholarship. This study was financed in part by the Coordenação de Aperfeiçoamento de Pessoal de Nível Superior - Brasil (CAPES) - Finance Code 001.

6. References

1. Togashi MM. Efeito do tamanho e distribuição de tamanho inicial das partículas da hematita, na cinética de sinterização assistida por micro-ondas [thesis]. São Carlos Universidade Federal de São Carlos; 2021.
2. Opuhovic O, Kareiva A. Historical hematite pigment: synthesis by an aqueous sol-gel method, characterization and application for the colouration of ceramic glazes. *Ceram Int.* 2015;41(3 Pt B):4504-13.
3. Muhajir M, Puspitasari P, Razak JA. Synthesis and applications of hematite α -Fe₂O₃: a review. *J Mech Eng Sci Technol.* 2019;3(2):51-8.
4. Luo Q, Nie F, Long X, Qiao Z, Yang G, Ma Y. Preparation of nanocrystalline α -Fe₂O₃ by radiation technique. *Curr Nanosci.* 2014;10:722-9.
5. Ramasami AK, Ravishankar TN, Sureshkumar K, Reddy MV, Chowdari BVR, Ramakrishna T et al. Synthesis, exploration of energy storage and electrochemical sensing properties of hematite nanoparticles. *J Alloys Compd.* 2016;671:552-9.
6. Mirzaei A, Janghorban K, Hashemi B, Bonyani M, Leonardi SG, Neri G. Highly stable and selective ethanol sensor based on α -Fe₂O₃ nanoparticles prepared by Pechini sol-gel method. *Ceram Int.* 2016;42:6136-44.
7. Luo Q, Nie F, Long X, Qiao Z, Yang G, Ma Y. Preparation of nano-Fe₂O₃ by CO₂-supercritical-process-assisted sol-gel method. *Curr Nanosci.* 2014;10:722-9.
8. Sun H, Zhang Y, Gong H, Li T, Li Q. Microwave sintering and kinetic analysis of Y₂O₃-MgO composites. *Ceram Int.* 2014;40:10211-5.
9. Menezes RR, Souto PM, Kiminami RHGA. Microwave sintering of ceramic materials. In: Lakshmanan A, editor. *Sintering of ceramics – new emerging techniques.* London: IntechOpen; 2012. p. 85-94.
10. Menezes RR, Souto PM, Kiminami RHGA. Microwave sintering of ceramics. Part I: fundamental aspects. *Ceramica.* 2017;53(325):1-10.
11. Rybakov KI, Olevsky EA, Semenov VE. The microwave ponderomotive effect on ceramic sintering. *Scr Mater.* 2012;66(12):1049-52.
12. Rybakov KI, Olevsky EA, Krikun EV. Microwave sintering: fundamentals and modeling. *J Am Ceram Soc.* 2013;96(4):1003-20.
13. Cheng J, Roy R, Agrawal D. Radically different effects on materials by separated microwave electric and magnetic fields. *Mater Res Innov.* 2002;5(3-4):170-7.
14. Lee S-W, Lee J-G, Chae K-P, Na S-Y. Superparamagnetic properties of γ -Fe₂O₃ nanoparticles. *J Korean Magn Soc.* 2010;20(5):196-200.
15. Togashi MM. Estudo da cinética de sinterização assistida por micro-ondas de pós cerâmicos nano e submicrométricos, com diferentes propriedades dielétricas [dissertation]. São Carlos Universidade Federal de São Carlos; 2017.
16. Han J, Mantas PQ, Senos AMR. Grain growth in Mn-doped ZnO. *J Eur Ceram Soc.* 2000;20(16):2753-8.
17. Gunnewiek RFK, Kiminami RHGA. Effect of heating rate on microwave sintering of nanocrystalline zinc oxide. *Ceram Int.* 2014;40:10667-75.
18. Liu Y, Ai Y, He W, Chen W, Zhang J. Grain growth kinetics in microwave sintered graphene platelets reinforced ZrO₂/Al₂O₃ composites. *Ceram Int.* 2018;44(14):16421-7.
19. Zuo F, Saunier S, Meunier C, Goeuriot D. Non-thermal effect on densification kinetics during microwave sintering of α -alumina. *Scr Mater.* 2013;69(4):331-3.
20. Zhu J, Ouyang C, Xiao S, Gao Y. Microwave sintering versus conventional sintering of NiCuZn ferrites. Part I: densification evolution. *J Magn Magn Mater.* 2016;407:308-13.
21. Togashi MM, Perdomo CPF, Kiminami RHGA. Densification kinetics of nano-hematite using microwave assisted dilatometry. *Ceram Int.* 2020;46:28546-60.
22. Croquesel J, Bouvard D, Chaix JM, Carry CP, Saunier S, Marinel S. Direct microwave sintering of pure alumina in a single mode cavity: grain size and phase transformation effects. *Acta Mater.* 2016;116:53-62.
23. Nuernberg RB, Morelli MR. Microwave assisted synthesis and sintering of Ba_{0.5}Sr_{0.5}Co_{0.8}Fe_{0.2}O_{3.8} perovskite. *Mater Res.* 2015;18(1):85-91.

24. Rahaman MN. Kinetics and mechanisms of densification. In: Fang ZZ, editor. Sintering of advanced materials. Oxford: Woodhead Publishing; 2010. p. 33-64. (Woodhead Publishing Series in Metals and Surface Engineering).
25. Du W, Ai Y, Chen W, He W, Zhang J, Fan Y et al. Grain growth kinetics and growth mechanism of columnar Al_2O_3 crystals in $\gamma\text{Nb}_2\text{O}_5$ -7.5 La_2O_3 - Al_2O_3 ceramic composites. Ceram Int. 2019;45(6):6788-94.